Energy 91 (2015) 1009–1017

Contents lists available at ScienceDirect

Energy

journal homepage: www.elsevier.com/locate/energy

Performance analysis of a thermoelectric air duct system for energy-efficient buildings

Kashif Irshad [a], Khairul Habib [a, *], Nagarajan Thirumalaiswamy [a], Bidyut Baran Saha [b, c]

[a] Department of Mechanical Engineering, Universiti Teknologi PETRONAS, 32610 Bandar Seri Iskandar, Perak Darul Ridzuan, Malaysia
[b] Kyushu University Program for Leading Graduate School, Green Asia Education Center, Interdisciplinary Graduate School of Engineering Sciences, Kyushu University, 6-1 Kasuga-koen, Kasuga-shi, Fukuoka 816-8580, Japan
[c] International Institute for Carbon-Neutral Energy Research (WPI-I2CNER), Kyushu University, Japan

A R T I C L E I N F O

Article history:
Received 10 April 2015
Received in revised form
24 July 2015
Accepted 30 August 2015
Available online xxx

Keywords:
Thermoelectric air duct system (TE-AD)
TRNSYS modeling
Thermoelectric cooling
Coefficient of performance
CO_2 emission
Carbon credit

A B S T R A C T

This paper describes experimental and simulation study results of an air duct system that cools down airflow by using TEMs (thermoelectric modules). This system is designated as TE-AD (thermoelectric air duct) system which consists of twenty four TEMs along with heat sink and fan for circulation of air. Both experimental and simulation results were in good agreement with each other and showed that the TE-AD system reduces room temperature in the range of 1.2–5.3 °C and humidity in the range of 5–31%. The COP (coefficient of performance) of the system ranges from 0.392 to 0.679 under different operating input current for Malaysian weather conditions. By comparing TE-AD system with conventional air conditioning system, energy saving of 38.83% and CO_2 emission mitigation of 38.81% was achieved with additional benefits of high reliability and refrigerant free system.

1. Introduction

Presently, maintaining thermal comfort has been a challenge for most of the developing countries, as the process of air conditioning in large buildings can lead to excessive use of energy [1]. Energy requirements for air conditioning will escalate from 300 TW h in the year 2000, to around 4000 TW h in the year 2050 and a further expected to increase around 10,000 TW h in 2100 [2]. One of the main reasons for higher energy requirement of an air conditioning system is 25–40% energy lost in an air duct system while channeling conditioned air inside the building [3]. Approaches to deal with the current situation are to utilize alternative energy sources and thus reduce the usage of regular power technologies and air conditioning system.

Thermo-electric effect was discovered at the beginning of the 19th century by Thomas Seebeck, and among the latest potential technologies being researched in compliance with the requirements of space conditioning [4]. TE materials are solid-state energy converters that can create a temperature difference when an electric potential is applied to the material (Peltier effect) or generates the electric potential by introducing a temperature difference (Seebeck effect) [5]. TE materials arranged in a certain configuration are called TEMs (thermoelectric modules) and it can be classified into either TEGs (thermoelectric generators), which directly convert heat to electricity, or thermoelectric coolers (TECs), which directly convert electricity into a temperature gradient [6]. Previously TEMs are limited only to small applications due low COP (coefficient of performance), but over the past few years researchers have identified its potential for building applications.

Stockolm et al. [7] in 1982 used TEMs for cooling small cabs of railroad and submarines. Lertsatitthanakorn et al. [8] investigate TE air-conditioning unit installed on the celling. Two heat exchanger one attached on the evaporator side were used to dissipate thermal energy from the source and other attached on the condenser side were used to discard heat to the surrounding environment. Result shows that at input current intensity of 3 A, cooling capacity of 169 W was achieved. Maneewan et al. [9] develop TE air conditioning system by implementing three TE modules for small space conditioning application. At operating current of 1 A, COP of 0.34 and cooling capacity of 29.2 W was achieved. Cosnier et al. [10] investigated air heating and cooling capacity of TEMs both

* Corresponding author. Tel.: +60 5 368 7146; fax: +60 5 365 6461.
E-mail address: khairul.habib@petronas.com.my (K. Habib).

http://dx.doi.org/10.1016/j.energy.2015.08.102
0360-5442/

Nomenclature

COP	Coefficient of Performance
G	Global solar radiation on a horizontal surface at the next hour (W/m^2 h)
G_N	Direct normal solar radiation at the next hour (W/m^2 h)
G_{TR}	Total radiation on surface at the next hour (W/m^2 h)
G_{BR}	Beam radiation on surface at the next hour (W/m^2 h)
G'	Geometric factor (area/length of TE element) (cm)
I	Input current to TEMS (A)
K_{TE}	The module's thermal conductance (W/K)
N	Total number of TE elements used in each module
n	Time in years
P_{TE}	Power input for TEM (W)
Q_{cold}	Heat absorbed at cold surface (W)
Q_{hot}	Heat released at hot surface (W)
RH	Relative humidity
RH_{in}	Indoor relative humidity
RH_o	Relative humidity of air at the outlet of air duct.
R_{TE}	The module's electrical resistance (Ω)
S_{TE}	The module's Seebeck Voltage (V/K)
TEM	Thermoelectric module
TE-AD	Thermoelectric air duct system
T_{cold}	Cold side temperature (K)
T_{hot}	Hot side temperature (K)
ΔT	$T_{hot} - T_{cold}$ (K)
T_{DB}	Dry-bulb temperature at the next time step (K)
T_{SKY}	Sky temperature at the next time step (K)
T_a	Ambient temperature at the next time step (K)
T_{in}	Indoor room temperature at the next time step (K)
T_o	Air duct outlet temperature at the next time step (K)
V_{in}	Voltage (V)
V_a	Velocity of air in duct at the next time step (m/s)
V_w	Wind velocity at the next time step (m/s)
V_f	Velocity of air exhausted into the room at the next time step (m/s)
W	Power consumption of fan (W)
Z	Figure of Meri (K$^{-1)}$
α	Seebeck Coefficient (V/K)
σ	Resistivity (Ω cm)
κ	Thermal conductivity (W/(cm K))
ρ	Humidity ratio at the next time step
φ	Solar azimuth and zenith angle
x	Range of measured value

experimentally and numerically. It was found that when the TE module was operated at the input electrical current supply of 4 A, cooling capacity of 50 W per module, with a temperature difference of 5 °C between hot and cold side and COP range between 1.5 and 2 was achieved. Li et al. [11] experimentally studied TE module application in cooling or heating of airflow for small envelope. Results showed that COP greater than 1.5 can be achieved with a small temperature difference of (5–10 °C) in cooling mode. Totala et al. [12] also attempted to study the effect of thermoelectric cooling in a 1 m^3 box using a single TEM and found that their design was able to cool the ambient air temperature from 32.5 °C to 22.1 °C using 4 TEMs, each providing 37.7 W of cooling power. Gillott et al. [13] investigated the effect of TEMs on small scale building space conditioning application. Results showed that maximum cooling capacity of 220 W and COP of 0.46 was achieved when TE cooling unit was operated at input electrical current supply of 4.8 A to each module. Shena et al. [14] use TEM as radiant panels instead of conventional hydronic panels to develop TE-RAC (thermo-electric radiant air-conditioning) system. This system can be used for both heating and cooling purpose and optimum results were obtained when the system operates at current 1.2 A. A Maximum COP of TE-RAC in the cooling mode was 1.77 and the minimum temperature achieved at cold side was 20 °C. Performance of TE air-conditioners were compared with conventional vapor compression air-conditioners by Riffat and Qiu [15]. Results showed that the COPs of TE air-conditioner was in the range of 0.3–0.45 while vapor compression air-conditioner was in the range of 2.6–3.0 respectively. However, Hermes and Barbosa [16] concluded that present TEMs was having only 1% thermodynamic efficiency as compared to Stirling and reciprocating vapor compression refrigeration systems which was having a 14% thermodynamic efficiency. So in order to improve performance of the TE air-conditioning system, Tipsaenporm et al. [17] applied direct evaporative cooling techniques in TE air-conditioning system, which enhances the cooling power from a value 53.0 W–74.5 W. Cherkez [18] develop a novel TE air-conditioning unit by combining TE and the Joule–Thomson effects. The results show that COP of system improves by a factor of 1.6–1.7 as compared to existing TE systems.

Different studies have shown that the application of TEMs for small scale air-conditioning system application has been achieved, but the application of same in an air duct for space conditioning of buildings has not been researched. The main significance of this paper is to study the application of TEMs in an air duct system for developing novel TE-AD (Thermoelectric air duct) system for large scale application. TE-AD system provides cool and dehumidified air to the test room and thus reduces cooling load and energy requirement. The prospect is not to have a fully air conditioned test room, but rather to have a thermally affordable house in the tropical climate of Malaysia without consuming excessive energy and refrigerants. In the present study, an experimental system containing TE-AD system was set up that cools down an airflow circulated through it. A simulation model using TRNSYS software that calculates the system's thermal performance was compared with the experimental system. First a description of the experimental setup, simulation model and results are presented followed by energy consumption, CO_2 emission and carbon credit potential by TE-AD system are illustrated.

2. Methodology

2.1. Test room description

The experiment and data collection was conducted from 1 January to 31 January 2015 using the single-room house facility equipped with TE-AD system located in the campus of Universiti Teknologi PETRONAS (4°23′11″N and 100°58′47″E, Perak, Malaysia). The test room is of dimensions 2.8 m (width, X) × 2.7 m (depth, Y) × 2.5 m (height, Z) as shown in Fig. 1 and its thermophysical properties are presented in Table 1. All the external walls are three-layered with a middle layer composed of 20 cm thick brick and both the side walls are plastered. The plaster thickness is 1.3 cm for the inside layer and 1.8 cm for outside layer. The Roof is covered by clay roof tiles. Gypsum board with 1.828 m × 1.219 m × 0.0063 m is used in the ceiling. The window on the north-west wall is 0.304 m high and 0.22 m wide and is made of plywood with a thickness of 2.2 cm. The windows have no

Fig. 1. Test room equipped with TE-AD.

rows and three columns (8 × 3). The columns were connected in parallel and TEMs in each column were internally connected in series. For each series, the positive wires of the TEMs were connected to the negative wires of the subsequent TEM while the positive wires at the end of each series were connected to a Bus bar (positive bar) and the negative wires at the end were connected to another Bus bar (negative bar). The positive bar was then connected to the positive terminal of the power supply, whereas the negative bar was attached to the negative terminal.

2.3. Experimental procedure

In order to provide sufficient cooling with the TE-AD system, suitable TEMs were selected to provide cooling load required by the test room. The test room peak cooling load which was 589 W, prior to installation of the air duct. It was noted that at an applied voltage of 5 V and input current of 6 A, each TEM module generates 25 W cooling power. Thus, for a cooling load of 589 W, the number of TEMs required was 24 units which can provide up to 600 W of cooling power at the given configuration, which was slightly higher than the required cooling load. The ambient air was circulated inside the test room via the TE-AD system installed on the north side of the room with the help of a fan as shown in Figs. 1 and 2. When

Table 1
Thermo physical properties of building material.

Material	Density (kg/m^3)	Specific heat (kJ kg^{-1} K^{-1})	Thermal conductivity (W m^{-1} K^{-1})
Brick tile	1892	0.88	0.798
Mud brick	1731	0.88	0.750
Soil	1622	0.88	0.519
Cement plaster	1762	0.84	0.721
Cement mortar	1648	0.92	0.719
Limestone tile	2420	0.84	1.800
Sand grave	2240	0.84	1.740
GI sheet	7520	0.50	61.060
Roof tile	2531	1.4253	0.632

overhangs over it. The test room has a single steel door is on the north-west wall of dimensions 2 m height and 0.821 m width. The door is made of 0.45 cm thick GI metal sheet.

2.2. Thermoelectric air duct description

The TE-AD as shown in Fig. 2 consists of an aluminum sheet housing supported by a frame and wrapped with insulation sheet. A Perspex sheet was installed at the center of the duct to house a total number of 24 (TEC1-12730) TEMs. It was designed to separate the air duct into two compartments where the air was cooled in one compartment and warmed in the other by the TEMs. A small hole was drilled in a Perspex sheet to bolt the heat sink and cooled object together using plastic screws. Dimensions of the aluminum heat sink are 65 mm × 65 mm × 20 mm and the aluminum cold plate is 65 mm × 65 mm × 10 mm. A thin layer coating of thermally conductive grease was applied on both hot and cold sides of TEMs for proper dissipation and absorption of heat into the surrounding medium. Both duct compartments were fitted with an exhaust fan of power 56 W, each to enhance the performance of the TE-AD system by controlling the velocity of the air flow in the duct. Both fans were connected to a speed controller to control the fan speed. The duct was insulated with an aluminum foil to prevent air leakage and thermal losses which might degrade the performance of the TE-AD system. Dimensions of the TE-AD system were accordance with ASHRAE Standard 62.2 [19,20] and the specifications are shown in Fig. 3. Twenty four TEMs were arranged in eight

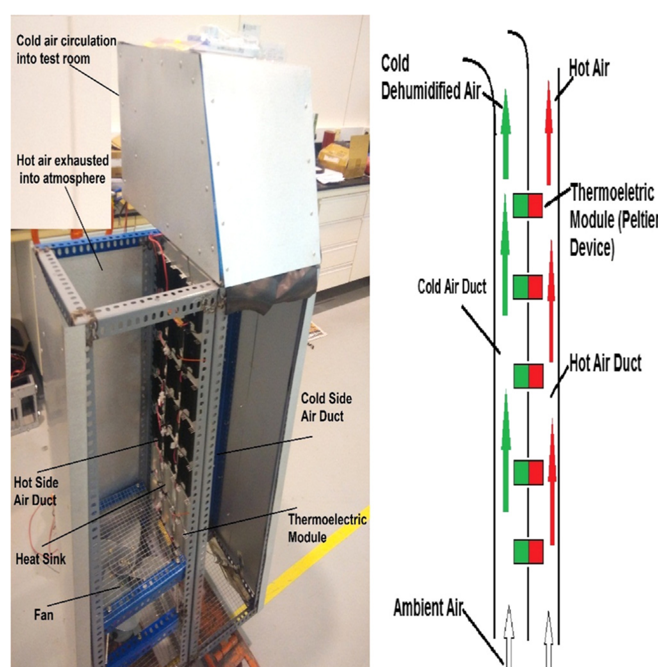

Fig. 2. Description of TE-AD.

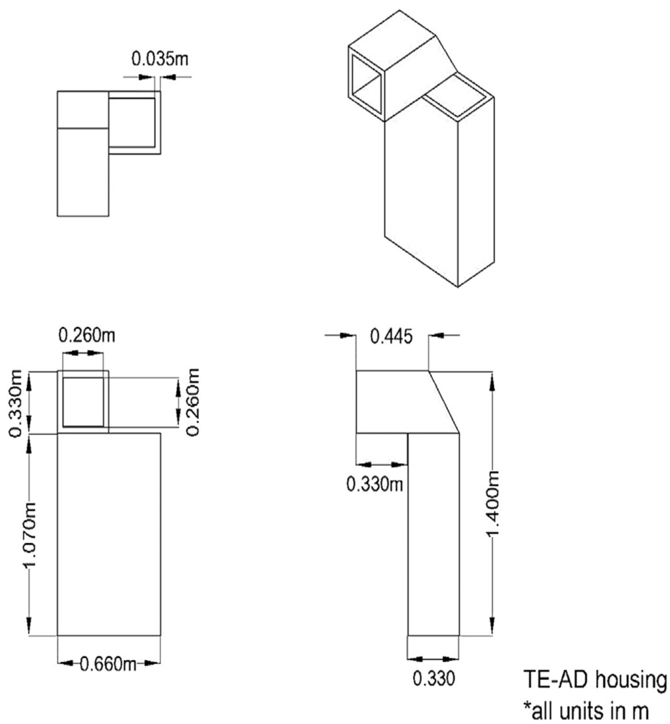

Fig. 3. Dimensional details of TE-AD.

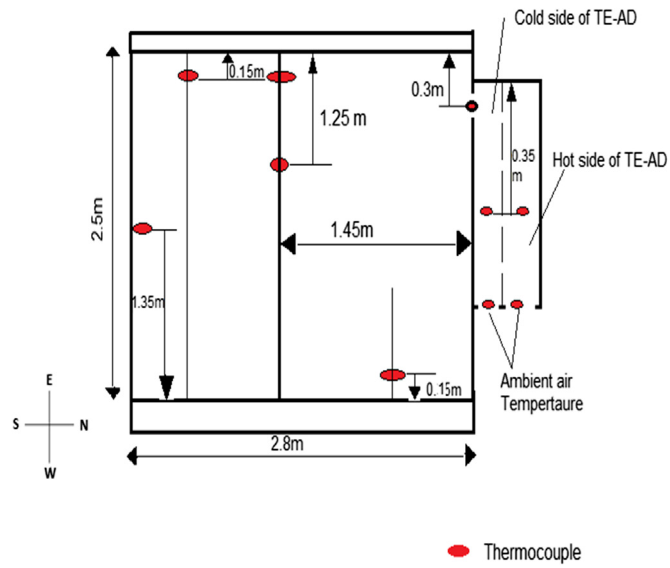

Fig. 4. Arrangement of thermocouple for temperature recording.

the DC power supply was turned on, a current was applied across the TEMs which created a temperature difference between the cold and hot sides of the module. The heat sinks attached to the hot side of the TEMs have eight fins, each 1 mm thick, 75 mm in length and 15 mm in height. In order to improve the heat transfer between the TEMs and the heat sinks, thermal paste was applied. The heat sinks were cooled by forced convection using an exhaust fan of power 56 W whose speed was adjusted by using a speed regulator.

The experiment was carried out by six levels of input current i.e. 2 A, 3 A, 4 A, 5 A, 6 A and 7 A was used to investigate the effect on main results i.e. indoor temperature, indoor relative humidity, COP, cooling capacity (Q_c), CO_2 emission and carbon credit potential. Ten K type thermocouples were fixed at different locations of the test room and TE-AD system as shown in Fig. 4, to collect the temperature data for every 5 min with the help of data loggers. The TE-AD system was run for four days at each level of input current. A portable solar meter was used to measure the solar irradiation at the time of operation of the TE-AD system. Table 2 shows the detail of the instruments employed in the experiment. An uncertainty analysis has been carried out and the results are presented in Table 3. It was found that solar radiation measurement has the largest relative uncertainty in the entire experiment. The values listed in Table 3 include all uncertainty sources and may be treated as the safest estimation of the uncertainty.

2.4. Simulation model

The system was modeled by using the dynamic simulation software TRNSYS (TRaNsient SYstem Simulation Program) v.17. This software can predict the thermal behavior of the test room, with a degree of flexibility and user–graphical interface [21]. Construction details and thermo physical properties of building materials are presented in Table 1. It was assumed that the heat transfer across the walls and roof is unidirectional and occurs along the thickness. The wall and roof structures were made of homogeneous material layers. Air change per hour was assumed to be constant and all thermal properties of building materials i.e. thermal conductivity and specific heat are assumed to be constant throughout the simulation study.

TRNSYS simulation modeling was defined by 10 modules (TYPE). The Information flow diagram of the system components presented in Fig. 5 has been drawn to show the interconnection between components and the flow of information between them. Each component is denoted by the box called TYPE. Each component requires a number of constant parameters and time dependent inputs in order to provide time dependent outputs. A given OUTPUT may be used as an INPUT to any number of other components.

The meteorological file contains the hourly data for a typical year was calculated using ambient conditions during three years (2012–2015) from the Malaysian Meteorological Department which include the ambient temperature, total radiation and wind speed. (Type 9a) data reader was installed to read the authentic weather data which was organized as a .txt file. This data consists of the ambient temperature, irradiation and the relative humidity that was accumulated from the weather station. Type 16 was used as radiation processor and Type 33, Type 69 was used for providing relative humidity, cloudiness factor, fictitious sky temperature data, and dry bulb temperature. Type 56 was used to model a single zone building with one air node for one zone. The Air node represents the thermal capacity of that particular zone and capacities that were associated. Distinct equipment modules can be coupled to the zones as either the internal convective gains or the ventilation fans. A separate pre-processing program PREBID that can read and execute a file having all building information as discussed above was used. PREBID generates two files that were used by the Type 56 component during a TRNSYS simulation. (Type 155) used to call a MALTAB routine into the TRNSYS and was a component created for calculating the temperature of the cold side of TEMs arranged in TE-AD as per equations (5)–(10). Specification of TEMs used in the simulation is given in Table 4. The temperature of the hot side of the module is assumed to be constant $T_{hot} = 25\ ^{\circ}C$.

Heating and cooling capacity of a TEM involved four types of heat i.e. Peltier cooling (Q_{PEC}), Peltier heating (Q_{PEH}), Joule heat (Q_{JH}) and Fourier heat (Q_{FH}) given as follows:

Table 2
Detail specification of equipment used in the experiment.

Apparatus	Type	Quantity	Function	Specification
Thermoelectric modules (TEMs)	Heibei TEC1-12730	24	To create a temperature gradient from an applied electric current	Maximum Current Input = 30.5 A @15 V Q_{max} = 257 W @T_h = 25 °C Q_{max} = 282 W @T_h = 50 °C
DC Power Supply	CPX400DP	1	To supply current into TEMs	Dual output, each with: 420 W, V_{max} = 60 V, I_{max} = 20A. Voltage and current draw can be adjusted.
Heatsinks	Finned Aluminum	24	To improve heat dissipation on hot side of TEM	
Anemometer		1	To measure air speed for controlling fan speed	
Thermocouple	Type-K	10	To measure temperature	Kept at 0 °C, measured accuracy within ±0.1 °C
Advanced Solar Power Meter		1	To measure solar irradiation	Resolution: 1 W/m^2 Spectral response: 400–1100 nm Accuracy ±2 W/m^2
Fan	HDEF-12 Exhaust Fan	2	To assist TE-AD by controlling air flow into the duct	230V, 56 W 9″ Diameter Speed = 1400 rpm Max air flow = 10–15 m^3/min
Data logger	midi Logger GL220	1	To record measured data	Every 10-min intervals record

Table 3
Uncertainty analysis of measured value.

Variable	Typical value (x)	Uncertainty (∂x)	Relative uncertainty ($\partial x/x$)%
T_In (°C)	18–35	0.1	0.56
T_a (°C)	20–40	0.1	0.55
T_C (°C)	15–25	0.1	0.67
T_H (°C)	25–40	0.1	0.4
Solarimeter (W/m$^{2)}$	100–900	2	2

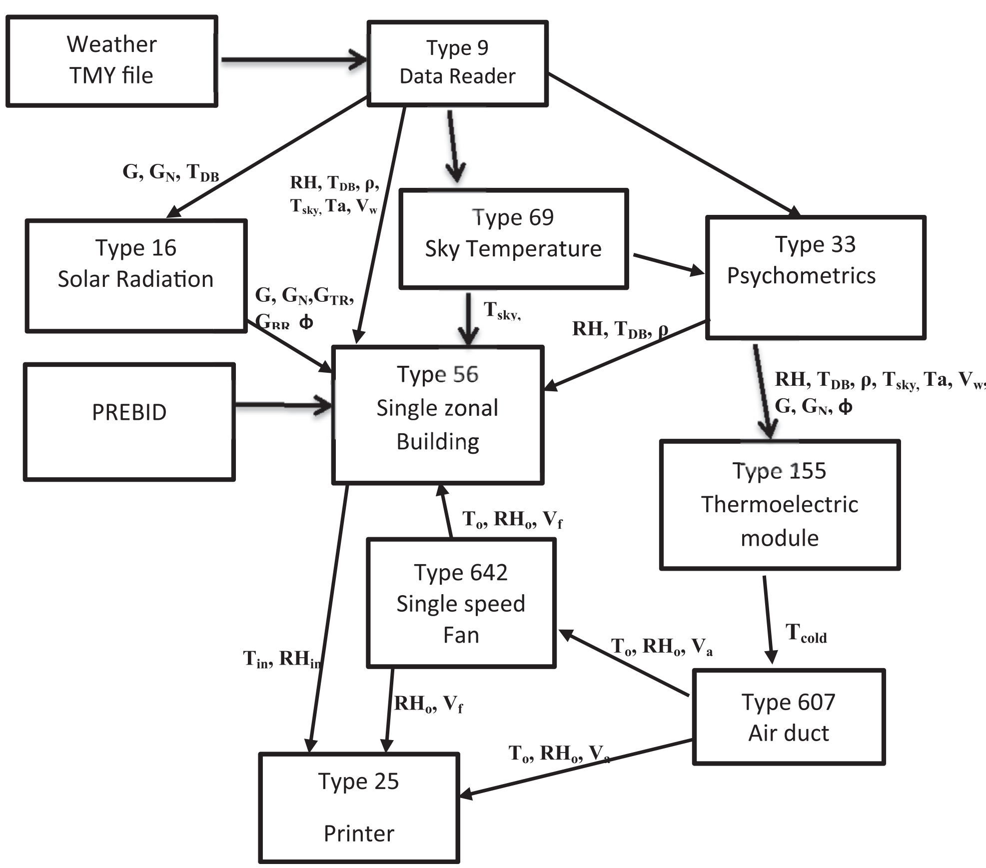

Fig. 5. TRNSYS information flow diagram.

Table 4
TE module properties.

Type	Dimension (mm)	N	I_{max} (A)	U_{max} (V)	Q_{cmax} (W)	T_{max} (°C)	R_{TE} (Ω)	S_{TE} (V/K)	K_{TE} (W/°C)
TEC 1-12730	62 × 62 × 4.8	127	30	15.4	266.7	68	0.27	0.051	0.5177

$$Q_{PEC} = S_{TE} I T_{cold} \quad (1)$$

$$Q_{PEH} = S_{TE} I T_{hot} \quad (2)$$

$$Q_{JH} = I^2 R_{TE} \quad (3)$$

$$Q_{FH} = K_{TE}(T_{hot} - T_{cold}) \quad (4)$$

By utilizing above four equation heating and cooling capacity of a TEM can be defined as:

$$Q_{cold} = S_{TE} I T_{cold} - 0.5 I^2 R_{TE} - K_{TE}\Delta T \quad (5)$$

$$S_{TE} = 2N\alpha \quad (6)$$

$$R_{TE} = 2N\sigma / G' \quad (7)$$

$$K_{TE} = 2N\kappa G' \quad (8)$$

$$Q_{hot} = S_{TE} I T_{hot} + 0.5 I^2 R_{TE} - K_{TE}\Delta T \quad (9)$$

$$V_{in} = (S_{TE} \times (T_{hot} - T_{cold})) + (I \times R_{TE}) \quad (10)$$

The electrical input power of a TEM is given by

$$P_{TE} = \alpha I (T_{hot} - T_{cold}) + I^2 R_{TE} \quad (11)$$

$$Z = \frac{S_{TE}^2}{R_{TE} K_{TE}} \quad (12)$$

The coefficient of performance under cooling mode of TEM can be given by

$$COP_{TE\ cooling} = \frac{Q_{cold}}{P_{TE}} \quad (13)$$

The system coefficient of performance in cooling mode is given by

$$COP_{TE-AD\ system} \frac{Q_{cold}}{(P_{TE} + W)} \quad (14)$$

(Type 607) was used to model the air duct. (Type 642) models a fan that was utilized to circulate the air through TE-AD. (Type 25) was a printer component used to output (or print) system variables at designated intervals of time.

3. Results and discussions

In this section, findings of implementation of the TE-AD system in the test room, operated at different input current are presented. The detailed discussion and comparison of experimental and simulation results are given in the subsequent subsections. Carbon credit potential and CO_2 emission mitigation by implementing the TE-AD system are also discussed.

3.1. Effects of the TE-AD system on room temperature

The effect of implementing the TE-AD system on indoor conditions of the test room at different input currents to TEMs is presented in Figs. 6–8. The TE-AD system was tested for six level of input current but only three significant curve is presented. When the TE-AD system was operated at 5 A, reduces indoor temperature and relative humidity in the range of 2.2–3.9 °C and 15–21% as presented in Fig. 6. It is depicted from Fig. 6 that the performance of the TE-AD system is highly dependent on the outside climatic condition (i.e. outside temperature and solar radiation intensity). Significant indoor temperature and relative humidity reduction were achieved during the initial and the final hour of operation of the TE-AD system when solar irradiance was below 300 W/m^2 and outside temperature was below 27 °C. During peak operating hour, the performance of the TE-AD system reduces as solar irradiance reaches above 850 W/m^2 and outside temperature to 34 °C. In order to improve the performance of the TE-AD system input current supply to TEMs was increased to 6A, which results in optimum indoor temperature reduction ranges between 2.8 and 5.3 °C and relative humidity reduction ranges between 20 and 31% as shown in Fig. 7. This is because with the increase in input current supply, the capacity of heat pumping of TEMs rises and more energy is absorbed on the cold side [18], while on the hot side more heat energy is released to the circulated air, causing rise in temperature of the hot side of TEMs. When ambient air comes in contact with the cooling side of TEMs that was lower than the dew point temperature of surrounding air, dry bulb temperature starts reducing. As the cooling process proceeds at some point it achieves the estimated dew point temperature of the air. At this point the water vapor contained in the air is reduced due to dew particles being formed on the ceramic surface of TEMs. Thus, temperature and humidity level of the air were reduced. On the hot side, where

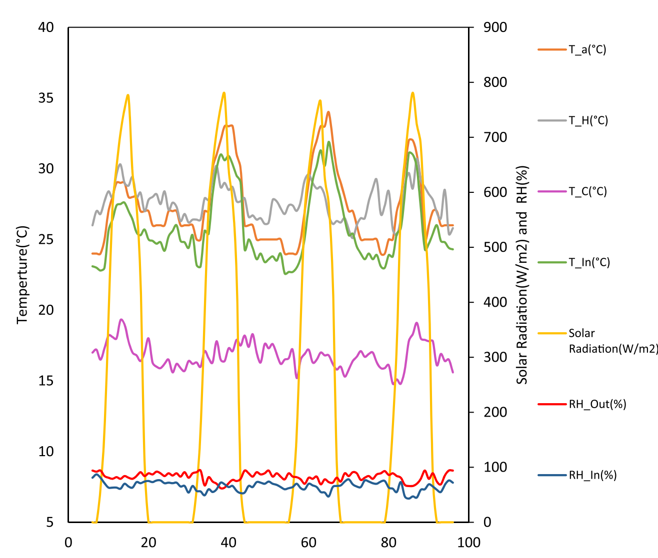

Fig. 6. Variation of indoor and outdoor climatic conditions of test room with time, when TE-AD system operated at 5A.

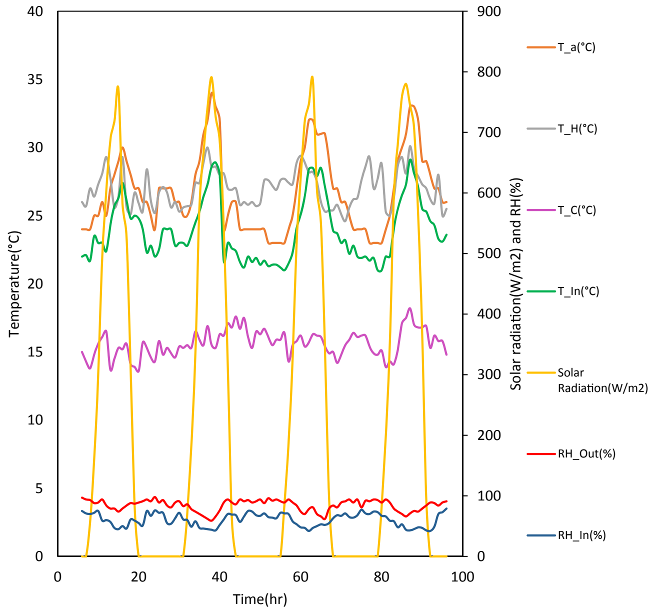

Fig. 7. Variation of indoor and outdoor climatic conditions of test room with time, when TE-AD system operated at 6A.

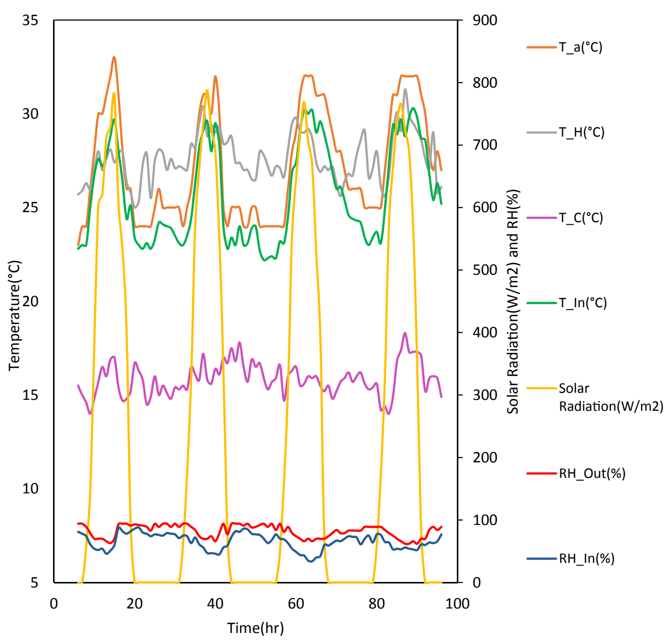

Fig. 8. Variation of indoor and outdoor climatic conditions of test room with time, when TE-AD system operated at 7A.

ambient air was allowed to circulate with a fan, this removes the heat dissipated from the TEMs and thus reduces Joule heat and thermal conductive energy presented in (Eqs. (3) and (4)) transferred back to the cold side. This causes an increase in the cooling capacity and net energy received at the cold side of TEMs. The Cold side of TEMs absorbs the heat from ambient air, thereby reducing its temperature. When this air is allowed to enter inside the test room it reduces its indoor temperature significantly. Interestingly, it was also found that as one increases the current supply from 6 A to 7 A the indoor temperature of the test room and hot side temperature of the TE-AD system increases as shown in Fig. 8. The reason for this behavior is explained in next section.

All the data obtained at different input current were fitted in the normal distribution. Goodness of fit test was observed by applying Pearson's chi-squared test. The calculated value of Pearson's chi-squared test for nearly all measured data come out to be less than or equal to 44 at 23 degrees of freedom and corresponding table value was 49.78 [22]. So the null hypothesis was rejected and the results were statically significant with 0.05 level of significance.

3.2. COP and cooling power of TE-AD system

The variation of cooling power and COP of the TE-AD system operated at different input currents is shown in Fig. 9. Results of the present study were compared with Maneewan et al. [9] results because of similar TEMs used for space conditioning purpose in both studies. It was found that as the input current increases, cooling power (Q_c) increases more than the temperature difference between the hot and cold side of the TEMs. Contrarily to results published by Ref. [13] these results showed that by controlling hot side temperature with the help of a fan, the COP increase from 0.392 to 0.679 and cooling power increases from 133.42 W to 498.78 W, with an increase in input current from 2 A to 6 A. Maximum COP and cooling power of the TE-AD system was achieved at 6 A, so the four day system operation reading at 6 A is presented in Fig. 10.

It is depicted from Fig. 10 that maximum COP and cooling capacity was achieved during the initial and final hour of operation of the TE-AD system. The trend follows by cooling capacity and COP was almost same and maximum COP and cooling capacity achieved was 0.679 and 498.6 W. As the experiment proceeds cooling capacity and COP decreased because of rise in surrounding temperature and increase in heat released rate by the TEMs. It was also found that when the current intensity was increased beyond 6 A, COP as well as cooling power decrease drastically as higher value of electrical current generates more heat, i.e. Joule heat which offset Peltier cooling effect. The fan becomes insufficient to carry away the heat and more joule heat and thermal conductive energy was transferred back to the cold side of TEMs. This reduces the cooling capacity of TEMs. Also, TE-AD systems when operating at higher current consume more energy, causing a decrease in maximum COP as shown in Fig. 9. Moreover Maneewan et al. [9] also support our results by finding that COP has a maximum increase for an input current of 2 A, and decreasing after that, in their case of small enclosure. By further comparing our results with previous TE cooling studies listed in Table 5, shows that the TE-AD system provide sufficient cooling capacity. A COP of the TE-AD system can

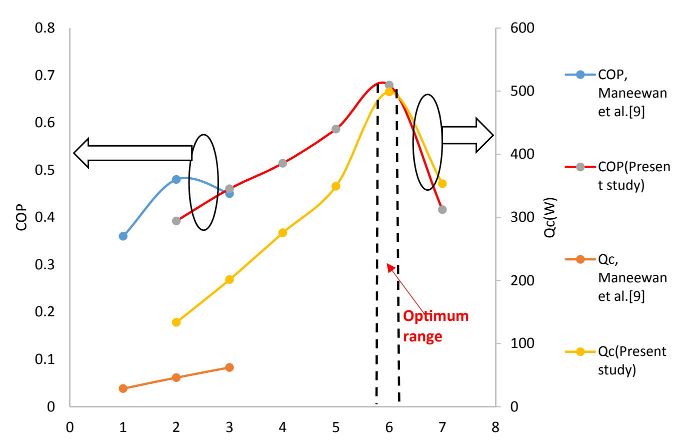

Fig. 9. Comparison of COP and cooling power of TE-AD system with previous study.

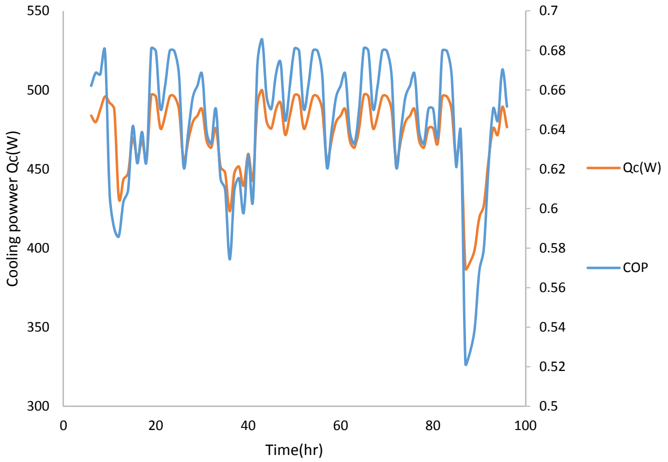

Fig. 10. Variation of COP and cooling capacity of test room with time, when TE-AD system operated at 6A.

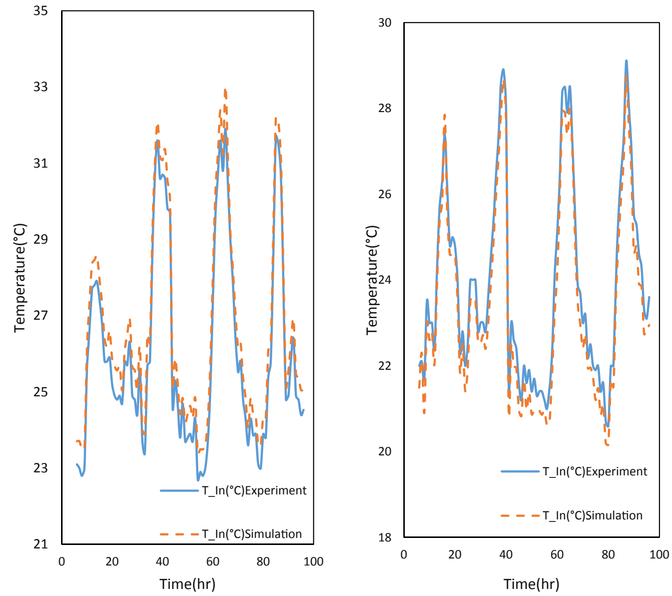

Fig. 11. Comparison of experimental and simulation data for indoor air temperature of test room when TE-AD system operated at 5A and 6A.

be further improved by implementing energy storage technologies i.e. integration of TE and phase change material (PCM), integration TE and solar technologies and integration of TE with energy recovery technologies.

3.3. *Comparison of simulation and experimental results*

The simulated and the experimental results of the TE-AD system were compared and found in good agreement. Since the optimum performance of the TE-AD system was found in the current range of 5–6 A, so experimental results of indoor temperature for this range were compared with simulated results and presented in Fig. 11. Results show that the temperature difference between experimental and simulation data was less than ±0.6 °C.

3.4. *Mitigation of CO_2 emissions and carbon credit potential*

The Malaysian building sector largely depends on air conditioners to provide thermal comfort to the occupants, which consumes lots of fossil fuel resources. Total CO_2 emissions in Malaysia have rapidly increased by 221% from year 1990–2004, and it is estimated to rise up to 328 million ton by 2020 [26]. TE-AD system is one of the most reliable and environmental friendly renewable energy technology which plays a significant role in CO_2 emissions mitigation. The numerical calculation was carried out to estimate the amount of CO_2 emission mitigated due to the existing TE-AD system as compared to conventional air conditioning systems. The average intensity of CO_2 discharge from coal thermal power plant in Malaysia is 1.21 kg/kWh [27]. The total mitigation of CO_2 emissions from the existing TE-AD system and conventional air conditioning systems for 20 years life can be calculated by using Eq. (14) [28] as follows:

$$\begin{aligned}&\mathrm{CO_2\ emission\ mitigated\ (kg/life)}\\&= 1.21\ \mathrm{kg/kWh)} \times E\ \mathrm{(kWh/year)} \times n\ \mathrm{(year)}\end{aligned} \qquad (15)$$

Comparison of electrical energy saving of test room mentioned above using the TE-AD and split air conditioner with a 1-ton-capacity was presented in Table 6. Room temperature and energy consumed by the air conditioner and TE-AD were recorded for a duration of 8-h/day. Energy consumption of TE-AD system was recorded when operating at 6 A while for split air conditioner when set point temperature is 24 °C. The set point temperature of room temperature for almost all office of Malaysian is in between 24 and 26 °C [28].

It was found that the total amount of CO_2 emissions due to existing TE-AD system in its life span is estimated as 57.17 tons which is 36.33 tons less as compared to conventional air conditioning system. Also TE-AD system consumes 1360.72 kWh/year less energy as compare to air conditioner unit.

The carbon credit potential of TE-AD system was determined on the basis of aggregate sum of CO_2 release mitigation from the system in its lifespan. The amount of carbon credit earned by TE-AD system can be calculated from the following Eq. (15) as follows [29],

Table 5
Comparison with pervious study on thermoelectric cooling.

Authors	Modules	Operation current (A)	COP	Cooling capacity (W)	Application area
Cosnier et al. [10]	Four piece (CP2-127-06L)	4–5	1.5	50 per module	Small enclosure
Maneewan et al. [9]	Three piece (TEC1-12708)	2	0.48	62.1	Compact TE air conditioner
Vian et al. [23]	Two pieces (6L)	~2.8	0.45	20	Small compartment
Gillot et al. [13]	Eight pieces (UT8-12-40-RTV)	4.8	0.46	220	Small space
Tipsaenporm et al. [17]	Three piece (TEC1-12708)	4.5	0.52	74.5	Compact TE air conditioner with Direct Evaporative Cooling System
Shen et al. [14]	(One piece TEC1-12706)	1.2	1.77	<5	Small space
Zhao et al. [24]	Fifteen pieces (RC12-8)	2.5	0.87	165	Small space conditioning with PCM integration.
Tan et al. [25]	Forty two (RC12-8)	5	0.78	1534.3	Space conditioning with PCM integration
Present work	Twenty four piece (TEC1-12708)	6	0.679	498.6	Test room of dimension 2.8 m × 2.7 m × 2.5 m

Table 6
Comparison of TE-AD system with air conditioning system.

Type of home	Energy consumption (kWh/year)	Emission of CO_2 (ton/life)	Energy saving (kWh/year)	CO_2 reduction (ton/life)
Room equipped with 1 ton split air conditioner	3504	93.54	0	0
Room equipped with Thermoelectric air duct	2143.28	57.17	1360.72	36.33

$$\text{Carbon credit earned} = \text{US\$}13/\text{ton} \times CO_2 \text{ emission mitigated by TE-AD system (tons/life)}. \quad (16)$$

In Eq (15) US$13/ton of CO_2 emission denotes the price value of one carbon credit for mitigation of 1 ton of CO_2 emission [30]. So the carbon credit potential of TE-AD system as compared to air conditioner system for its life span is around US$ 472.29.

4. Conclusions

A novel TE-AD system was successfully installed and tested for the test room. Major conclusions can be drawn as follows:

1. COP over 0.679 and cooling power, Q_c up to 499 W could be achieved in an air-cooling mode with the system operated in the range of 5–6 A, and 5 V.
2. Temperature difference between indoor and the outdoor of the test room can be reach up to 3.0–5.3 °C while operating at 6 A current intensity. Fan and heat sink attached to the hot side of TEMs plays an important role in maintaining the temperature difference between the hot and the cold side of TEMs as small as possible, by dissipating heat generated at the hot side of TEM to the outside environment.
3. By increasing electrical intensity above 6 A, the cooling performance of the TE-AD system was reduced as heat starts transferring from hot to cold side of the TEMs.
4. Experimental results were compared with the simulation data and it was observed that the temperature differences between indoor and outdoor conditions of the test room were below 6%.
5. CO_2 emission mitigation due to existing TE-AD system as compared to a conventional air conditioning system in its life span is estimated 36.33 tons. The TE-AD system consumes 1360.72 kWh/year less energy as compared to the conventional air conditioner unit and carbon credit potential of the TE-AD system for its life span is around US$ 472.29.

The TE-AD system having a low COP than the conventional air conditioning system, but can be used for space conditioning purpose for the less fluctuating environment. This system can also be coupled with the duct or air distribution system of the air conditioning systems, thereby reduces air-duct system losses and enhances the cooling performance of the system. The system performance can further be improved by optimizing TEMs figure-of-merit (ZT value), reducing the heat transfer resistance of the hot side of TEMs, using energy storage material such as PCM, reducing air flow obstruction by redesigning fins of the heat sink and integrating with a photovoltaic system.

References

[1] Habib K, Choudhury B, Chatterjee PK, Saha BB. Study on a solar heat driven dual-mode adsorption chiller. Energy 2013;63:133–41.
[2] Isaac M, van Vuuren DP. Modeling global residential sector energy demand for heating and air conditioning in the context of climate change. Energy Policy 2009;37:507–21.
[3] Fisk WJ, Delp W, Diamond R, Dickerhoff D, Levinson R, Modera M, et al. Duct systems in large commercial buildings: physical characterization, air leakage, and heat conduction gains. Energy Build 2000;32:109–19.
[4] Bell LE. Cooling, heating, generating power, and recovering waste heat with thermoelectric systems. Science 2008;321:1457–61.
[5] Enescu D, Virjoghe EO. A review on thermoelectric cooling parameters and performance. Renew Sustain Energy Rev 2014;38:903–16.
[6] Tsai HL, Lin JM. Model building and simulation of thermoelectric module using Matlab/Simulink. J Electron Mater 2010;39:2105–11.
[7] Stockolm JG, Pujol-Soulet L, Sternat P. Prototype thermoelectric air conditioning of a passenger railway coach,. In: 4th Intern Conf on Thermoelectric Energy Conversion, Arlington, TX, USA; 1982.
[8] Lertsatitthanakorn C, Hirunlabh J, Khedari J, Daguenet M. Experimental performance of a ceiling-type free convicted thermoelectric air conditioner. Int J Ambient Energy 2002;23(2):173–7.
[9] Maneewan S, Tipsaenprom W, Lertsatitthanakorn C. Thermal comfort study of a compact thermoelectric air conditioner. J Electron Mater 2010;39:1659–64.
[10] Cosnier M, Fraisse G, Luo L. An experimental and numerical study of a thermoelectric air-cooling and air-heating system. Int J Ref 2008;31:1051–62.
[11] Li T, Tang G, Gong G, Zhang G, Li N, Zhang L. Investigation of prototype thermoelectric domestic-ventilator. Appl Therm Eng 2009;29:2016–21.
[12] Totala NB, Gangopadhyay D. Study and fabrication of thermoelectric air cooling and heating system. Int J Eng Invent 2014;4:20–30.
[13] Gillott M, Jiang L, Riffat S. An investigation of thermoelectric cooling devices for small-scale space conditioning applications in buildings. Int J Energy Res 2010;34:776–86.
[14] Shen L, Xiao F, Chen H, Wang S. Investigation of a novel thermoelectric radiant air-conditioning system. Energy Build 2013;59:123–32.
[15] Riffat SB, Qiu G. Comparative investigation of thermoelectric air-conditioners versus vapour compression and absorption air-conditioners. Appl Therm Eng 2004;24:1979–93.
[16] Hermes CJL, Barbosa JR. Thermodynamic comparison of Peltier, Stirling, and vapor compression portable coolers. Appl Energy 2012;91:51–8.
[17] Tipsaenporm W, Lertsatitthanakorn C, Bubphachot B, Rungsiyopas M, Soponronnarit S. Improvement of cooling performance of a compact thermoelectric air conditioner using a direct evaporative cooling system. J Electron Mater 2012;41(6):1186–92.
[18] Cherkez R. Theoretical studies on the efficiency of air conditioner based on permeable thermoelectric converter. Appl Therm Eng 2012;38:7–13.
[19] Walker IS, Sherman MH. Energy implications of meeting ASHRAE standard 62.2. ASHRAE Trans 2008;114:505–21.
[20] ASHRAE. ASHRAE handbook – HVAC applications. 2007.
[21] Chen TY. A method for the direct generation of comprehensive numerical solar building transfer functions. Sol Energy 2003;74:123–32.
[22] Agresti A, Kateri M. Categorical data analysis. Int Encycl Stat Sci 2014:206–8.
[23] Vián JG, Astrain D. Development of a thermoelectric refrigerator with two-phase thermosyphons and capillary lift. Appl Therm Eng 2009;29:1935–40.
[24] Zhao D, Tan G. Experimental evaluation of a prototype thermoelectric system integrated with PCM (phase change material) for space cooling. Energy 2014;68:658–66.
[25] Tan G, Zhao D. Study of a thermoelectric space cooling system integrated with phase change material. Appl Therm Eng 2015;86:187–98.
[26] Shamsuddin AH. Development of renewable energy in Malaysia-Strategic Initiatives for carbon reduction in the power generation sector. Procedia Eng 2012;49:384–91.
[27] Shafie SM, Masjuki HH, Mahlia TMI. Life cycle assessment of rice straw-based power generation in Malaysia. Energy 2014;70:401–10.
[28] Saidur R. Energy consumption, energy savings, and emission analysis in Malaysian office buildings. Energy Policy 2009;37:4104–13.
[29] Chel A, Tiwari GN, Chandra A. Simplified method of sizing and life cycle cost assessment of building integrated photovoltaic system. Energy Build 2009;41:1172–80.
[30] California Carbon Dashboard, 2015. [Online]. Available: http://calcarbondash.org/. (accessed 04.2015).